

Fluctuations in superconducting rings with two order parameters

Jorge Berger¹ and Milorad V. Milošević²

¹*Department of Physics and Optical Engineering,
Ort-Braude College, P.O. Box 78, 21982 Karmiel, Israel*

²*Departement Fysica, Universiteit Antwerpen, Groenenborgerlaan 171, B-2020 Antwerpen, Belgium*

Starting from the Ginzburg–Landau energy functional, we discuss how the presence of two order parameters and the coupling between them influence a superconducting ring in the fluctuative regime. Our method is exact, but requires numerical implementation. We also study approximations for which some analytic expressions can be obtained, and check their ranges of validity. We provide estimates for the temperature ranges where fluctuations are important, calculate the persistent current in MgB₂ rings as a function of temperature and enclosed flux, and point out its additional dependence on the cross-section area of the ring. We find temperature regions in which fluctuations enhance the persistent currents and regions where they inhibit the persistent current. The presence of two order parameters that can fluctuate independently always leads to larger averages of the order parameters at T_c , but only for appropriate parameters this yields larger persistent current. In cases of very different material parameters for the two coupled condensates, the persistent current is inhibited.

PACS numbers: 74.78.Na, 74.40.-n

I. INTRODUCTION

Fluctuations are extremely important near phase transitions, and have therefore been the subject of intense research in the past. Particularly in superconductivity, it has been shown that thermally driven electronic fluctuations, i.e. formation and dissociation of Cooper pairs close to the critical temperature T_c , can affect all relevant properties of a superconductor.¹ Techniques that incorporate thermal fluctuations to the Ginzburg–Landau model are described in a recent review.² Fluctuations in mesoscopic loops are particularly interesting because their critical temperature is reduced in an oscillatory fashion as a function of the magnetic field—a phenomenon known as the Little–Parks (LP) effect.³ More importantly, as LP oscillations are directly related to flux (vorticity) entry in superconductors, one can identify the magnetic fields for which fluctuations are particularly important, as is the case of half-integer flux values.⁴ The latter experiment⁴ detected current in the ring above T_c , a clear signature of fluctuations, and may be regarded as a paradigm for thin superconducting ring behavior, a case for which the theory for thermal fluctuations is known exactly.⁵ The additional influence of quantum fluctuations was addressed in Ref. 6.

Superconductivity is essentially a macroscopic quantum state with long-range phase coherence, therefore described as a single wave function. Superconductors with several order parameters have recently attracted great attention due to the discovery of MgB₂ and high T_c superconductivity in pnictides. In such cases, thermal excitation allows contributions from multiple wave functions and one may expect a dramatically different behavior of the system. With that as motivation, we here explore the interplay of the wave functions and thermal fluctuations in superconducting rings with two order parameters. The rings we will consider need not be made of a two-band

superconductor, but may also consist of two thin superimposed superconducting rings,⁷ possibly separated by an isolating layer, such as the active part in readily made experiments with annular Josephson junctions.⁸

We conduct our theoretical analysis in the framework of the Ginzburg–Landau (GL) theory. The multiband GL equations were developed long ago;⁹ in the case of two bands the free energy density has the form

$$f = \sum_{\nu=1,2} \left(\tilde{a}_{\nu} |\tilde{\Delta}_{\nu}|^2 + \frac{\tilde{b}_{\nu}}{2} |\tilde{\Delta}_{\nu}|^4 + \tilde{K}_{\nu} |\mathbf{\Pi} \tilde{\Delta}_{\nu}|^2 \right) - \tilde{\gamma} (\tilde{\Delta}_1 \tilde{\Delta}_2^* + \tilde{\Delta}_2 \tilde{\Delta}_1^*), \quad (1)$$

where $\tilde{\Delta}_{1,2}$ are the order parameters, $\tilde{a}_{1,2}$, $\tilde{b}_{1,2}$, $\tilde{K}_{1,2}$ and $\tilde{\gamma}$ are material parameters and $\mathbf{\Pi} = \nabla + 2\pi i \mathbf{A} / \Phi_0$, with \mathbf{A} the vector potential and Φ_0 the superconducting flux-quantum. Zhitomirsky and Dao¹⁰ obtained expressions for the material parameters in a multiband superconductor using Gor'kov's technique. Kogan and Schmalian¹¹ recently emphasized that consistency imposes conditions on the temperature dependence of these coefficients, which results in the same coherence length for both order parameters in a two-band superconductor. Shanenko *et al.*¹² went on to show the importance of terms of higher order in temperature, and the resulting separation of characteristic lengths for the two bands. We should note, however, that fluctuations move the order parameters astray from equilibrium, so that in general their ratio is not constant. Moreover, besides two-band superconductors, we are interested in relating our results to additional systems, where the coefficients in Eq. (1) may have a different temperature dependence. In this paper we thus adopt the standard GL approach, where the material parameters in Eq. (1) are arbitrary functions of the temperature and any required restriction will be a particular case.

II. METHOD

In this paper we deal with one dimensional superconducting rings with two order parameters, extending the results obtained by von Oppen and Riedel⁵ from single to two order parameters. Instead of the formalism of Ref. 5, we will follow a slightly different approach, which in our view is conceptually simpler. We start by absorbing the coefficients $K_{1,2}$ into the order parameters and by switching to a gauge invariant formulation, i.e. we define

$$\Delta_\nu(\theta) = \exp\left(\frac{2\pi i R}{\Phi_0} \int_0^\theta A(\theta') d\theta'\right) \sqrt{\tilde{K}_\nu} \tilde{\Delta}_\nu(\theta), \quad (2)$$

where R is the radius of the ring, θ is the angle along the ring and A is the tangential component of \mathbf{A} . Likewise we define

$$a_\nu = \frac{\tilde{a}_\nu}{\tilde{K}_\nu}, \quad b_\nu = \frac{\tilde{b}_\nu}{\tilde{K}_\nu^2}, \quad \gamma = \frac{\tilde{\gamma}}{\sqrt{\tilde{K}_1 \tilde{K}_2}}. \quad (3)$$

With these definitions the free energy density becomes

$$f = \sum_{\nu=1,2} \left(a_\nu |\Delta_\nu|^2 + \frac{b_\nu}{2} |\Delta_\nu|^4 + \frac{1}{R^2} \left| \frac{d\Delta_\nu}{d\theta} \right|^2 \right) - \gamma (\Delta_1 \Delta_2^* + \Delta_2 \Delta_1^*). \quad (4)$$

With the normalizations we are using, $a_\nu^{-1/2}$ is the coherence length for the order parameter Δ_ν in the absence of coupling to the other order parameter. As in Ref. 5, we consider a uniform 1D ring, which in particular does not alter the applied field (screening is negligible), so that no magnetic energy has to be added to f .

In order to have a more intuitive picture of the problem, we represent the complex order parameters Δ_ν by two-dimensional real vectors \mathbf{r}_ν , such that in polar coordinates $r_\nu = |\Delta_\nu|$ and the angular coordinate ϑ_ν is the phase of Δ_ν . Integrating f over the volume of the ring, its free energy becomes

$$F = \frac{2w}{R} \int_{-\pi}^{\pi} d\theta \left(\frac{1}{2} \left| \frac{d\mathbf{r}_1}{d\theta} \right|^2 + \frac{1}{2} \left| \frac{d\mathbf{r}_2}{d\theta} \right|^2 + V \right), \quad (5)$$

where w is the cross section of the ring and

$$V = \frac{R^2}{2} \left(a_1 r_1^2 + a_2 r_2^2 + \frac{b_1}{2} r_1^4 + \frac{b_2}{2} r_2^4 - 2\gamma r_1 r_2 \cos(\vartheta_1 - \vartheta_2) \right). \quad (6)$$

As in Ref. 5, $\mathbf{r}_{1,2}(\theta)$ may be regarded as the trajectories of two fictitious particles during a period of time $-\pi \leq \theta \leq \pi$. The first two terms in the integrand of Eq. (5) then represent their kinetic energy and V their potential energy.

Following Ref. 13, a pair of functions $\mathbf{r}_\nu(\theta)$ is interpreted as a microstate of the system and F as the energy

of the system for that microstate. It follows that up to an irrelevant multiplicative constant the partition function is

$$Z = \int \mathcal{D}\mathbf{r}_1 \mathcal{D}\mathbf{r}_2 \exp(-F/k_B T), \quad (7)$$

where T is the temperature and $\int \mathcal{D}\mathbf{r}_1 \mathcal{D}\mathbf{r}_2$ denotes integration over all functions $\mathbf{r}_\nu(\theta)$ with appropriate periodicity. Since $\tilde{\Delta}_\nu$ are single valued, $r_\nu(\theta = \pi) = r_\nu(\theta = -\pi)$ and $\vartheta_\nu(\theta = \pi) = \vartheta_\nu(\theta = -\pi) + 2\pi\varphi$, where φ is the flux enclosed by the ring divided by Φ_0 .

Using slight adaptations of Eqs. (2.14), (2.15), (2.16), (2.22) and (2.23) in Ref. 13, Z can be brought to the form

$$Z = \sum_n \exp(-2\pi\varepsilon_n/S) \times \int d\mathbf{r}_1 d\mathbf{r}_2 \Psi_n^*[\mathbf{r}_\nu(\theta = \pi)] \Psi_n[\mathbf{r}_\nu(\theta = -\pi)]. \quad (8)$$

Here ε_n and $\Psi_n[\mathbf{r}_\nu]$ are a complete set of eigenvalues and normalized eigenfunctions of the fictitious Hamiltonian

$$H = -\frac{S^2}{2} (\nabla_1^2 + \nabla_2^2) + V, \quad (9)$$

where the Laplacian ∇_ν^2 acts on \mathbf{r}_ν and $S = k_B T R / 2w$. S has dimensions of surface in the plane of the trajectories of $\mathbf{r}_{1,2}$ and dimensions of force in reality. The integral in Eq. (8) is taken over the entire planes of motion for each particle, but for every argument \mathbf{r}_ν in Ψ_n we have to take the corresponding argument in Ψ_n^* .

We note now that the angular momentum operator $L_z = -i(\partial/\partial\vartheta_1 + \partial/\partial\vartheta_2)$ commutes with H . We can therefore choose the set of eigenfunctions $\{\Psi_n\}$ with well defined angular momentum, i.e. they can obey $L_z \Psi_{n,\ell} = \ell \Psi_{n,\ell}$ and therefore have the form $\Psi_{n,\ell}(\mathbf{r}_1, \mathbf{r}_2) = \sum_{\ell_1} \psi_{n,\ell,\ell_1}(r_1, r_2, \vartheta_1 - \vartheta_2) \exp[i(\ell_1 \vartheta_1 + (\ell - \ell_1) \vartheta_2)]$, with ℓ and ℓ_1 integers. In view of the periodicity conditions of \mathbf{r}_ν , it follows $\Psi_{n,\ell}[\mathbf{r}_\nu(\theta = \pi)] = \exp(2\pi i \ell \varphi) \Psi_{n,\ell}[\mathbf{r}_\nu(\theta = -\pi)]$. By substitution of this result into Eq. (8) we obtain

$$Z = \sum_\ell \exp(-2\pi i \ell \varphi) Z_\ell, \quad (10)$$

with

$$Z_\ell = \sum_n \exp(-2\pi\varepsilon_{n,\ell}/S), \quad (11)$$

where summation in Eq. (10) is made over all integers and in Eq. (11) over all the states with total angular momentum ℓ . Since H is invariant under the transformation $\{\vartheta_1, \vartheta_2\} \rightarrow \{-\vartheta_1, -\vartheta_2\}$, $\varepsilon_{n,-\ell} = \varepsilon_{n,\ell}$ and we can also write

$$Z = Z_0 + 2 \sum_{\ell=1}^{\infty} \cos(2\pi\ell\varphi) Z_\ell. \quad (12)$$

Once the partition function is known, all the equilibrium quantities can be derived from it. The average current around the ring is

$$\langle I \rangle = \frac{k_B T}{\Phi_0} \frac{\partial \ln Z}{\partial \varphi} = -\frac{k_B T}{\Phi_0} \frac{4\pi}{Z} \sum_{\ell=1}^{\infty} \sin(2\pi\ell\varphi) \ell Z_{\ell}. \quad (13)$$

Following similar steps to those that led to Eq. (12), we obtain that the statistical average of any function of the absolute values of the order parameters is

$$\langle p(|\Delta_1|, |\Delta_2|) \rangle = \frac{1}{Z} \left[P_0 + 2 \sum_{\ell=1}^{\infty} \cos(2\pi\ell\varphi) P_{\ell} \right], \quad (14)$$

where $P_{\ell} = \sum_n \exp(-2\pi\varepsilon_{n,\ell}/S) \langle n\ell | p(r_1, r_2) | n\ell \rangle$. Here we introduced the matrix element $\langle n\ell | p(r_1, r_2) | n\ell \rangle = \int d\mathbf{r}_1 d\mathbf{r}_2 p(r_1, r_2) |\Psi_{n,\ell}(\mathbf{r}_\nu)|^2$, which may in practice be evaluated in any convenient basis.

III. EVALUATIONS

A. High temperature

Let T be sufficiently higher than T_c , so that the order parameters are small and the quartic terms in V can be neglected. For high T we can also assume $a_1 + a_2 > \sqrt{(a_1 - a_2)^2 + 4\gamma^2}$ and define the quantities

$$\eta = \frac{a_1 - a_2}{2\sqrt{(a_1 - a_2)^2 + 4\gamma^2}}, \quad (15)$$

$$\xi_{3,4}^2 = \frac{2}{a_1 + a_2 \mp \sqrt{(a_1 - a_2)^2 + 4\gamma^2}}.$$

For $\gamma = 0$ and $a_1 > a_2$, $\xi_{3,4} = a_{2,1}^{-1/2}$; we therefore regard $\xi_{3,4}$ as a sort of coherence lengths in the presence of coupling.

We can now define a rotation in the 4D space of both particles through

$$\mathbf{r}_1 = \sqrt{\frac{1}{2} - \eta} \mathbf{r}_3 - \sqrt{\frac{1}{2} + \eta} \mathbf{r}_4,$$

$$\mathbf{r}_2 = \sqrt{\frac{1}{2} + \eta} \mathbf{r}_3 + \sqrt{\frac{1}{2} - \eta} \mathbf{r}_4. \quad (16)$$

With this transformation, the ‘‘potential energy’’ in Eq. (6) becomes

$$V_{\text{quad}} = (R^2/2)[(r_3/\xi_3)^2 + (r_4/\xi_4)^2]. \quad (17)$$

The following features should be noted: (i) in the coordinates $\{\mathbf{r}_3, \mathbf{r}_4\}$, $\nabla_1^2 + \nabla_2^2$ still has the meaning of the Laplacian in the 4D space; (ii) since on passing from $\theta = -\pi$ to $\theta = \pi$ both ϑ_1 and ϑ_2 increase by $2\pi\varphi$, and since $\mathbf{r}_{3,4}$ are linear combinations of $\mathbf{r}_{1,2}$ with fixed coefficients, also their angles $\vartheta_{3,4}$ increase by $2\pi\varphi$; (iii) the angular momentum operators $-i\partial/\partial\vartheta_{3,4}$ for each separate particle now both commute with the Hamiltonian;

(iv) the total angular momentum equals the sum of the angular momenta of each particle and the total energy equals the sum of their energies. As a consequence of these features, the partition function in Eq. (10) becomes $Z = Z^{(3)}Z^{(4)}$, where $Z^{(\nu)}$ is the value of Z obtained when $\varepsilon_{n,\ell}$ is replaced with the value that corresponds to particle ν only. It follows that equilibrium quantities such as the average current or the average energy will equal the sum of the separate contributions of particles 3 and 4.

The Hamiltonian of the fictitious particles 3 and 4 is just that of two decoupled harmonic oscillators and its eigenvalues are well known: $\varepsilon_{n,\ell}^{(3,4)} = (SR/\xi_{3,4})(2n + |\ell| + 1)$. The sum in Eq. (11) becomes a geometric series and we obtain

$$Z_{\ell}^{(3,4)} = \frac{e^{-2\pi|\ell|R/\xi_{3,4}}}{2 \sinh 2\pi R/\xi_{3,4}}. \quad (18)$$

Substitution into Eq. (10) gives

$$Z^{(3,4)} = [2(\cosh 2\pi R/\xi_{3,4} - \cos 2\pi\varphi)]^{-1} \quad (19)$$

and the average current in the ring equals

$$\langle I_{\text{quad}} \rangle = - (2\pi \sin 2\pi\varphi k_B T / \Phi_0) [(\cosh 2\pi R/\xi_3 - \cos 2\pi\varphi)^{-1} + (\cosh 2\pi R/\xi_4 - \cos 2\pi\varphi)^{-1}]. \quad (20)$$

From Eq. (20) we can obtain the Little–Parks temperature, i.e., the temperature for the onset of superconductivity in the absence of fluctuations. Without fluctuations the current vanishes above this onset; this is implemented by taking the limit $k_B T \rightarrow 0$ in the first factor in Eq. (20). At the LP temperature the current becomes nonzero, requiring divergence of the second factor, i.e. $iR/\xi_3 = \varphi \pmod{1}$. From here, the LP condition is

$$R^2[\sqrt{(a_1 - a_2)^2 + 4\gamma^2} - (a_1 + a_2)] = 2\varphi^2, \quad (21)$$

where for simplicity of notation we restrict ourselves to the range $|\varphi| \leq 1/2$. Near T_c we can write $a_\nu = a_{\nu c} - \alpha_\nu \tau$, with $\tau = (T_c - T)/T_c$ and $a_{1c}a_{2c} = \gamma^2$; if in addition $(\varphi/R)^2 \ll \alpha_{1,2}$, condition (21) is fulfilled for

$$\tau = \tau_{\text{LP}} = \frac{a_{1c} + a_{2c}}{a_{1c}\alpha_2 + a_{2c}\alpha_1} \frac{\varphi^2}{R^2}. \quad (22)$$

B. Hartree approximation

In the potential given by Eq. (6) we now make the replacement $(b_{1,2}/2)r_{1,2}^4 \rightarrow b_{1,2}\langle r_{1,2}^2 \rangle r_{1,2}^2$. At high temperatures both terms are negligible and at low temperatures, where fluctuations can be neglected, they both lead to the same ‘‘force’’ $-\nabla V$.¹⁷

With this approximation the potential becomes again quadratic, so that we can still use the results of the previous section by substituting $\eta \rightarrow \eta'$ and $\xi_{3,4} \rightarrow \xi'_{3,4}$,

with

$$\begin{aligned} \eta' &= \frac{a'_1 - a'_2}{2\sqrt{(a'_1 - a'_2)^2 + 4\gamma^2}}, \\ \xi_{3,4}^{\prime 2} &= \frac{2}{a'_1 + a'_2 \mp \sqrt{(a'_1 - a'_2)^2 + 4\gamma^2}}, \\ a'_{1,2} &= a_{1,2} + b_{1,2}\langle r_{1,2}^2 \rangle. \end{aligned} \quad (23)$$

In order to implement this approximation, we have to evaluate $\langle r_{1,2}^2 \rangle$. $\langle r_{3,4}^2 \rangle$ are given by

$$\begin{aligned} \langle r_{3,4}^2 \rangle &= -\frac{S\xi_{3,4}' \partial \ln Z^{(3,4)}}{2\pi R^2 \partial(1/\xi_{3,4}')} \\ &= \frac{S\xi_{3,4}'}{R} \frac{\sinh 2\pi R/\xi_{3,4}'}{\cosh 2\pi R/\xi_{3,4}' - \cos 2\pi\varphi}; \end{aligned} \quad (24)$$

on the other hand, since $\langle \mathbf{r}_3 \cdot \mathbf{r}_4 \rangle = 0$, $\langle r_{1,2}^2 \rangle = (1/2 \mp \eta')\langle r_3^2 \rangle + (1/2 \pm \eta')\langle r_4^2 \rangle$, hence $\langle r_{3,4}^2 \rangle = (1/2 \mp 1/4\eta')\langle r_1^2 \rangle + (1/2 \pm 1/4\eta')\langle r_2^2 \rangle$. Substituting this into Eq. (24) leads to

$$\begin{aligned} \left(\frac{1}{2} \mp \frac{1}{4\eta'}\right) \langle r_1^2 \rangle + \left(\frac{1}{2} \pm \frac{1}{4\eta'}\right) \langle r_2^2 \rangle &= \\ \frac{S\xi_{3,4}'}{R} \frac{\sinh 2\pi R/\xi_{3,4}'}{\cosh 2\pi R/\xi_{3,4}' - \cos 2\pi\varphi}. \end{aligned} \quad (25)$$

This is a system of two equations for obtaining $\langle r_1^2 \rangle$ and $\langle r_2^2 \rangle$.

For a general situation, Eqs. (25) have to be solved numerically, but we can find asymptotic expressions for some special situations of interest. Sufficiently above the critical temperature T_c one usually has $2\pi R/\xi_{3,4}' \gg 1$, so that the fractions at the right of Eqs. (25) reduce to 1. Near T_c and for a range in which $b_\nu \langle r_\nu^2 \rangle \ll \alpha_\nu |\tau| \ll a_\nu$ we obtain

$$\begin{aligned} \langle |\Delta_{1,2}|^2(T) \rangle &= \langle r_{1,2}^2 \rangle \approx \\ \frac{k_B T}{2(a_{1c} + a_{2c})^{3/2} w} &\left(a_{1c,2c} + \frac{a_{2c,1c}(a_{1c} + a_{2c})}{\sqrt{(a_{1c}\alpha_2 + a_{2c}\alpha_1)|\tau|}} \right) \end{aligned} \quad (26)$$

It is interesting to note that $\langle |\Delta_{1,2}|^2(T) \rangle$ decreases very moderately with $T - T_c$. If the radius of the ring is sufficiently large, we still have $2\pi R/\xi_{3,4}' \gg 1$ at $T = T_c$; assuming that $b_\nu \langle r_\nu^2 \rangle \ll a_\nu$ still holds leads to

$$\begin{aligned} \langle |\Delta_{1,2}|^2(T_c) \rangle &\approx \left(\frac{a_{2c,1c}^2 k_B^2 T_c^2}{4(a_{1c} + a_{2c})\beta_{1,2} w^2} \right)^{1/3} \\ &+ \frac{a_{1c,2c}[3\beta_{1,2} - a_{2c,1c}(b_1 + b_2)]k_B T_c}{6(a_{1c} + a_{2c})^{3/2}\beta_{1,2} w}, \end{aligned} \quad (27)$$

with $\beta_{1,2} = b_{1,2}a_{2c,1c} + b_{2,1}a_{1c,2c}^3/\gamma^2$. Comparison of Eqs. (26) and (27) with the values of $|\Delta_{1,2}|^2$ in the absence of fluctuations enables us to estimate the range of temperatures for which fluctuations are important.

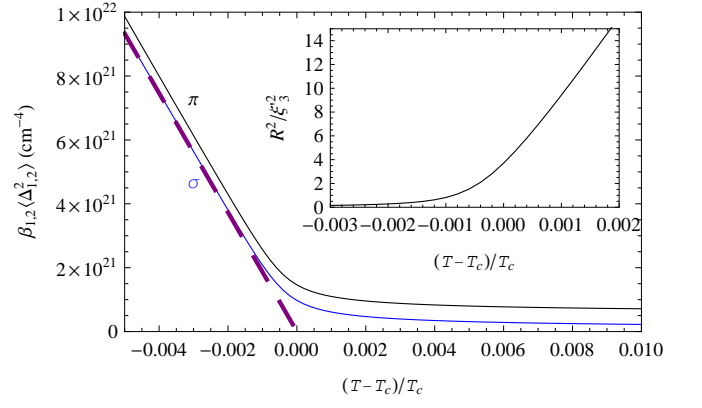


FIG. 1: Average Cooper-pair densities $|\Delta_{\nu=1,2(=\sigma,\pi)}|^2$ in the ring as a function of temperature, calculated in the Hartree approximation. Each $|\Delta_\nu|^2$ has been multiplied by β_ν for the purpose of comparison with the values in the absence of thermal fluctuations (dashed line). The sample is a ring of radius 10^{-4} cm and cross section 10^{-10} cm² that encloses no magnetic flux. The material parameters are those of MgB₂, taken from Ref. 14. Inset: $(R/\xi_3')^2$ for the same ring.

Figure 1 shows the values of $\langle \Delta_{1,2}^2 \rangle = \langle r_{1,2}^2 \rangle$ near T_c for MgB₂, using the material parameters reported in Ref. 14. In the absence of thermal fluctuations, $\beta_{1,2}\langle \Delta_{1,2}^2 \rangle$ is given by the dashed line for both bands. The inset in the figure shows the behavior of R/ξ_3' near T_c ; $\xi_4' \ll \xi_3'$ remains practically constant in this range.

C. Exact evaluation

We define the basis Hamiltonian

$$H_B(k_1, k_2) = -\frac{S^2}{2} (\nabla_1^2 + \nabla_2^2) + \frac{R^2}{2} (k_1^2 r_1^2 + k_2^2 r_2^2), \quad (28)$$

which has the known set of eigenfunctions

$$\begin{aligned} \psi_{n_1, \ell_1, n_2, \ell_2}(\mathbf{r}_1, \mathbf{r}_2) &= C \prod_{\nu=1,2} r^{\ell_\nu} e^{-Rk_\nu r_\nu^2/2S} \\ &\times {}_1F_1(-n_\nu, |\ell_\nu| + 1, Rk_\nu r_\nu^2/S) e^{i\ell_\nu \vartheta} \end{aligned} \quad (29)$$

with eigenvalues $RS[k_1(2n_1 + |\ell_1| + 1) + k_2(2n_2 + |\ell_2| + 1)]$. Here C is the normalization constant and ${}_1F_1$ is Kummer's hypergeometric function. We can then evaluate any matrix element $H_{i,j} = \langle \psi_i | H | \psi_j \rangle$, where the functions $\psi_{i=1,\dots,N}$ are the functions with lowest eigenvalues within the basis of the Hilbert space provided by Eq. (29). More precisely, when evaluating Z_ℓ , we include in the set $\{\psi_i\}$ only eigenfunctions that obey $\ell_1 + \ell_2 = \ell$. If N is sufficiently large, then the lowest eigenvalues of the matrix $(H_{i,j})$ will be a sufficiently accurate approximation for the lowest eigenvalues of the operator H . In practice, rather than fixing N , we fix maximum values for n_1 , $|\ell_1|$, n_2 and $|\ell_2|$.

We are interested in choosing k_1 and k_2 so that an accurate approximation is obtained without N becoming

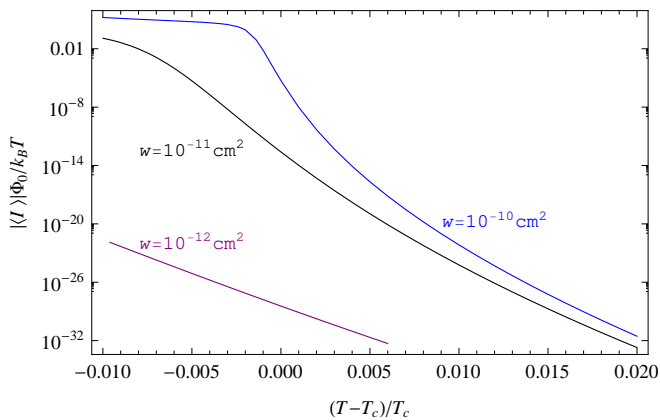


FIG. 2: Average current in a two-order-parameter superconducting ring as a function of temperature. For the top curve the parameters are as in Fig. 1, except that the normalized flux is $\varphi = 0.25$. For the lower curves the cross section w of the ring is smaller. The current was evaluated using a truncated basis of the Hilbert space, provided by the functions in Eq. (29) with maximum quantum numbers $n_{1,\max} = 11$, $|\ell_{1,\max}| = 22$, $n_{2,\max} = 4$, and $|\ell_{2,\max}| = 8$.

prohibitively large. From Eq. (29) we see that the scale of $\langle r_\nu^2 \rangle$ is given by S/Rk_ν ; we therefore set $k_\nu = pS/R\langle r_\nu^2 \rangle$, where $\langle r_\nu^2 \rangle$ is obtained from the Hartree approximation and p is still a free parameter. Since for a good approximation the eigenvalues should actually be independent of p , we mimic this situation by minimizing the lowest eigenvalue of $(H_{i,j})$ with respect to p .

Figure 2 shows the currents as functions of the temperature obtained with this method for rings of three different cross sections, with the material parameters of MgB_2 . For completeness, the figure includes also values of current that are too small to be experimentally observable. The temperature range covered here is much wider than the range presented in Ref. 5, where the temperature scale is given by the Thouless correlation energy (divided by k_B) which is of the order of the LP temperature; for a MgB_2 ring with radius of the order of a micron the LP temperature is of the order of $10^{-5} T_c$.

For sufficiently high temperature (the required temperature decreases with cross section w), the current becomes independent of the cross section. For the parameters taken here and $T = 3T_c$, a ring with $w = 10^{-10} \text{ cm}^2$ and a ring with $w = 10^{-8} \text{ cm}^2$ carry the same average current (within 1% difference). At the other extreme, far below T_c , i.e. where fluctuations are unimportant, $\langle I \rangle \propto w$. However, the dependence of $\langle I \rangle$ on w near T_c is not intermediate: we notice in Fig. 2 that decrease of w by an order of magnitude near T_c leads to a current decrease of several orders of magnitude, whereas for intermediate behavior the current would decrease by one order of magnitude at most. Figure 3 shows the scaled current against the scaled temperature for the same rings as in Fig. 2, close to T_c . We notice that, in spite of the moderate influence of temperature on $\langle |\Delta_{1,2}|^2 \rangle$ predicted

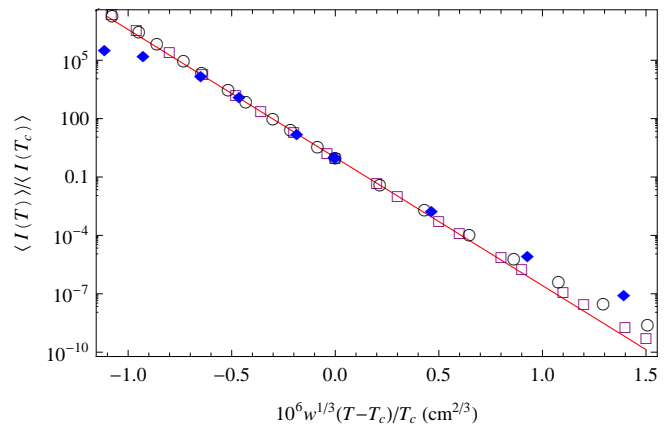


FIG. 3: Scaling of the function $\langle I(T) \rangle$ with the cross section. The parameters are the same as in Fig. 2. \blacklozenge : $w = 10^{-10} \text{ cm}^2$; \circ : $w = 10^{-11} \text{ cm}^2$; \square : $w = 10^{-12} \text{ cm}^2$. The straight line is a guide for the eye.

by Eq. (26), the current decreases exponentially. We also find that for smaller cross sections the rate of change of $\langle I \rangle$ is slower. We empirically found that the scaling $w^{1/3}$ leads to a universal curve.

We attribute didactic interest to understanding the behavior of our methods far below T_c . There, convergence of the series in Eqs. (12) and (13) becomes slow, and numeric implementation of the exact evaluation becomes inefficient. Below certain temperature, $\xi_3'^2$ in Eq. (23) becomes negative, and interpretation of the potential in Eq. (17) as that of a harmonic oscillator, and the sum of convergent geometric series that led to Eqs. (20) and (25) is no longer justified. Nevertheless, the expressions in Eqs. (20) and (25) are analytic functions of $\xi_3'^2$, than remain meaningful and are expected to remain valid beyond the range in which they were proven. Numeric implementation of the Hartree approximation requires special care in order to pick the relevant rather than spurious solutions of Eqs. (25). In the limit $T \rightarrow 0$, $R/\xi_3' \rightarrow i\varphi$, so that the right hand side in the first of Eqs. (25) does not vanish. Taking the appropriate limits in Eqs. (20) and (25) we obtain that the current in the Hartree approximation is $I_H(0) = -4\pi w(\Delta_1^2 + \Delta_2^2)\varphi/R\Phi_0$, exactly as in the absence of fluctuations.

We conclude this section with a review of the accuracy of our evaluations. The accuracy of the “exact” evaluation can be estimated by repeating it with reduced maximum values for n_ν and $|\ell_\nu|$. We found the largest inaccuracy for large w and small T . In the results presented in Fig. 2, the maximal inaccuracies are of the order of 10%. Figure 4 compares our approximation methods against the exact evaluation for $w = 10^{-10} \text{ cm}^2$. One can see in the figure that all the approximation methods are very inaccurate precisely in the most interesting region, i.e., close to T_c . The range of temperatures where the approximations are inaccurate is larger for smaller cross-sections w . Note also that there exists a range of temperatures for which the mean field current is larger than

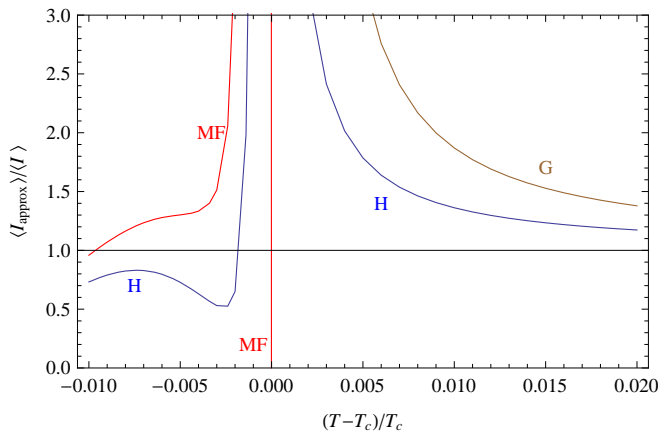


FIG. 4: Ratio of the current values obtained with approximated methods to the exact evaluation. Parameters are the same as in Fig. 1, except that here $\varphi = 0.25$. G: Gaussian (quadratic) approximation; H: Hartree approximation; MF: mean field evaluation (i.e., without fluctuations). The descent of the MF curve to 0 at the Little–Parks temperature looks vertical in this scale.

our exact evaluation, meaning that thermal fluctuations *inhibit the current* in this region.

IV. INDEPENDENCE AND ASYMMETRY OF THE ORDER PARAMETERS

The most conspicuous qualitative differences of a two order parameter system, as compared to a system with a single order parameter, are *independence* and *asymmetry*. By independence we mean that at a given point and time the two order parameters are not necessarily equal to each other; by asymmetry we mean that the average values of the order parameters are not necessarily the same. In this section we investigate the influence of these properties.

A. Symmetric case

We start by considering independence while assuming equal coefficients for both order parameters. For simplicity, we assume

$$a_\nu = \gamma - \alpha\tau, \quad b_\nu = b, \quad (30)$$

with γ , α and b constants. As an illustration, we may think of a film of a uniform single-parameter material of thickness z_0 with energy density $-2\alpha\tau|\Delta|^2 + b|\Delta|^4 + 2|\nabla\Delta|^2$. If we decide to denote by Δ_1 (resp. Δ_2) the value of Δ in the upper (resp. lower) half of the film, substitute the z -derivative by a finite difference and average over z_0 , we obtain the energy density $-\alpha\tau(|\Delta_1|^2 + |\Delta_2|^2) + b(|\Delta_1|^4 + |\Delta_2|^4)/2 + |\nabla_{xy}\Delta_1|^2 + |\nabla_{xy}\Delta_2|^2 + (8/z_0^2)(|\Delta_1|^2 + |\Delta_2|^2 - \Delta_1\Delta_2^* - \Delta_2\Delta_1^*)$, with

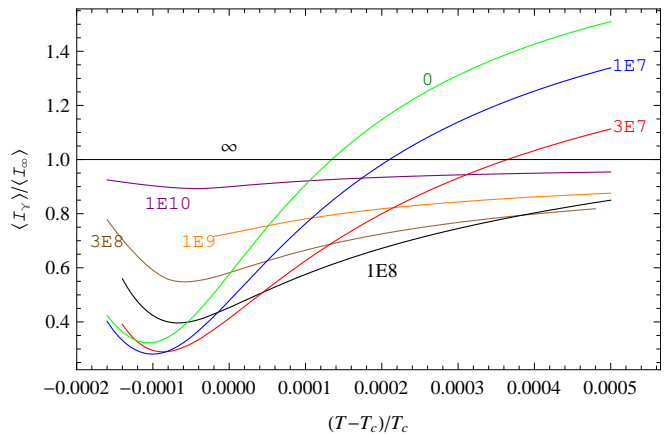


FIG. 5: Comparison among currents as functions of the temperature for systems with different coupling γ , but with otherwise identical parameters. The value of γ is marked next to every curve in E-notation (e.g. 3E7 denotes $\gamma = 3 \times 10^7 \text{ cm}^{-2}$). The other parameters are $R = 10^{-4} \text{ cm}$, $w = 10^{-10} \text{ cm}^2$, $\alpha = 10^{12} \text{ cm}^{-2}$, $b = 10^{17} \text{ erg}^{-1} \text{ cm}^{-1}$, $k_B T_c = 10^{-15} \text{ erg}$, $\varphi = 0.25$.

∇_{xy} being the component of the gradient in the plane of the film. One can easily identify that we have recovered the energy density for two order parameters, with coupling $\gamma = 8/z_0^2$. In the limit $z_0 \rightarrow 0$, $\gamma \rightarrow \infty$, and Δ_1 and Δ_2 are the same; in the opposite extreme, $\gamma \rightarrow 0$, and Δ_1 and Δ_2 are independent, while in the general case they are correlated. Following this analogy, it is very easy to obtain results for the cases $\gamma \rightarrow 0$ and $\gamma \rightarrow \infty$: the case $\gamma \rightarrow 0$ is equivalent to that of two single parameter systems in parallel, and the case $\gamma \rightarrow \infty$ is equivalent to that of a single parameter system with a doubled cross section.

Figure 5 compares calculated average currents $\langle I(T) \rangle$ as the parameter γ is varied in the range $0 \leq \gamma < \infty$, while all the other parameters are common to all curves. For a facilitated comparison, all the functions have been divided by $\langle I_\infty(T) \rangle$, the current obtained for $\gamma \rightarrow \infty$. Figure 5 shows the temperature range close to T_c ; far below T_c the influence of fluctuations is negligible and all the curves should coalesce. For every temperature, we note that as γ increases from 0 to ∞ , $\langle I(T) \rangle$ changes from $\langle I_0(T) \rangle$ to $\langle I_\infty(T) \rangle$. However, this change is not monotonic: $|\langle I(T) \rangle|$ initially decreases and after reaching a minimum increases towards $|\langle I_\infty(T) \rangle|$. The fact that $|\langle I_0(T) \rangle| < |\langle I_\infty(T) \rangle|$ for $T \approx T_c$ may look surprising, since $\gamma = 0$ means larger freedom than $\gamma \rightarrow \infty$ and we would therefore expect larger fluctuations in the former case. We will see in the following that indeed the order parameters assume larger values for $\gamma = 0$; however, they may be less coordinated, resulting in a smaller current.

The solid curves in Fig. 6 show the values of φ for which the current is maximum at $T = T_c$ for the limiting cases $\gamma = 0$ and $\gamma \rightarrow \infty$. From a dimensional analysis we find that in the present situation the temperature enters the operator H/S only through the combination $k_B T_c b R^3 / w$,

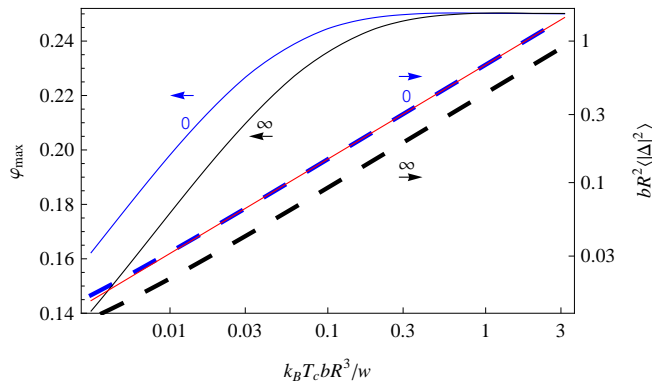


FIG. 6: Magnetic flux for which the fluctuation current is maximal, and value of the order parameters at $T = T_c$, as functions of T_c . $\langle|\Delta|^2\rangle$ was evaluated at $\varphi = \varphi_{\max}$. Each curve is marked by its value of γ and by an arrow that points to the relevant y -axis. The thin straight line (red online) highlights the asymptotic power dependence of $bR^2\langle|\Delta|^2\rangle$ on $k_B T_c b R^3 / w$.

so that φ_{\max} is a function of this quantity. Since the mean field current has its maximum at $\varphi_{\max} > 1/4$, it is interesting to note that φ_{\max} can be smaller than $1/4$. The curve for $\gamma \rightarrow \infty$ can be inferred from the case $\gamma = 0$: in order to obtain it at a given T_c , we have to double the value of w . Since φ_{\max} is a function of $k_B T_c b R^3 / w$, doubling w is the same as dividing T_c by 2, i.e., at a given T_c , the value of φ_{\max} for $\gamma \rightarrow \infty$ is the same that φ_{\max} for $\gamma = 0$ had at half that temperature. With a logarithmic x -axis, this relation gives a shift of the curve to the right.

The dashed lines in Fig. 6 show the values of $bR^2\langle|\Delta|^2\rangle$ at $T = T_c$ and $\varphi = \varphi_{\max}$, evaluated by means of Eq. (14). Except for $k_B T_c \ll w/bR^3$ or $k_B T_c \gg w/bR^3$, we obtain $\langle|\Delta|^2\rangle \approx 0.68(bR^2)^{-1}(k_B T_c b R^3 / w)^{2/3} = 0.68(k_B^2 T_c^2 / bw^2)^{1/3}$ for $\gamma = 0$. For $\gamma \rightarrow \infty$ $\langle|\Delta|^2\rangle$ is smaller by a factor $2^{2/3}$. The first term in the Hartree approximation value in Eq. (27) is smaller than the result obtained for $\gamma \rightarrow \infty$ by about 7%.

Figure 7 shows the average current evaluated at $T = T_c$ and $\varphi = \varphi_{\max}$. As already found in Ref. 5, $\langle I(T_c) \rangle$ is not a monotonic function of T_c , but has a maximum instead. As discussed above, the curve for $\gamma \rightarrow \infty$ is obtained as a shift of the curve for $\gamma = 0$. What we learn from this curve is that for $k_B T_c < 0.163w/bR^3$ $|\langle I_0(T_c) \rangle| > |\langle I_\infty(T_c) \rangle|$, meaning that independence of the order parameters *enhances* the fluctuation current, whereas the *opposite* occurs for $k_B T_c > 0.163w/bR^3$.

B. Asymmetric case

There are three material parameters that can differ between the order parameters: $a_{1c} \neq a_{2c}$, $\alpha_1 \neq \alpha_2$ and $b_1 \neq b_2$. Since near T_c the usual case is $|\alpha_{1,2}\tau|, b_{1,2}|\Delta_{1,2}|^2 \ll |a_{1c} - a_{2c}|$, we focus on the influence of the difference

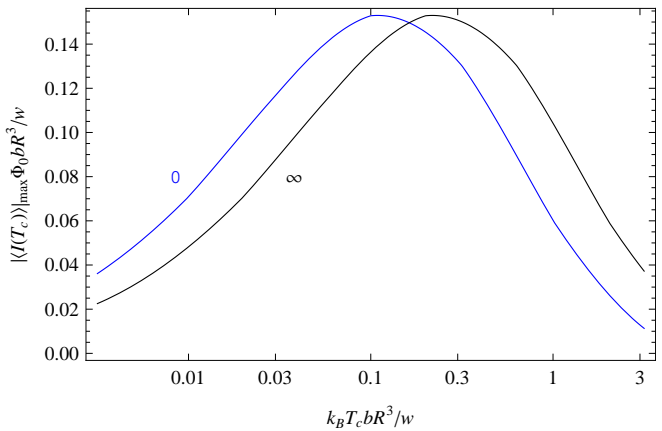


FIG. 7: Maximum current at $T = T_c$ as a function of the scaled T_c for $\gamma = 0$ and for $\gamma \rightarrow \infty$.

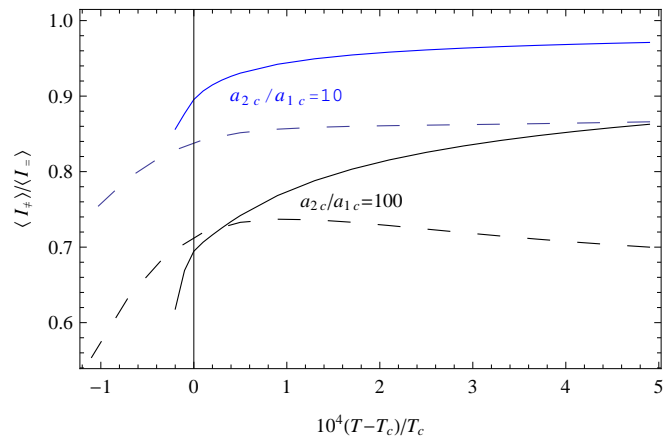


FIG. 8: Ratio between the fluctuation currents for the case $a_{1c} \neq a_{2c}$ (denoted I_{\neq}) and the case $a_{1c} = a_{2c}$ (denoted $I_{=}$). For the solid lines $b = 3 \times 10^{15} \text{ erg}^{-1} \text{ cm}^{-1}$ ($k_B T_c b R^3 / w = 0.03$) and $\gamma = 3 \times 10^6 \text{ cm}^{-2}$; for the dashed lines $b = 10^{17} \text{ erg}^{-1} \text{ cm}^{-1}$ ($k_B T_c b R^3 / w = 1$) and $\gamma = 3 \times 10^7 \text{ cm}^{-2}$. In all cases $\varphi = \varphi_{\max}$. The other parameters are the same as in Fig. 5.

between a_{1c} and a_{2c} .

Figure 8 shows the ratio between the fluctuation currents for the cases $a_{1c} \neq a_{2c}$ and $a_{1c} = a_{2c}$, while all the other parameters are kept unchanged. Although the values of $k_B T_c b R^3 / w$ and γ do have some influence, the general trend is that the difference between a_{1c} and a_{2c} inhibits fluctuation supercurrent in the region $T \approx T_c$, with this effect being stronger for $T < T_c$.

V. CONCLUSIONS

Motivated by recent surge in interest in the physics of coupled condensates in two-band superconductors, we have analyzed the role and importance of fluctuations in superconducting rings with two order parameters. We have extended the analysis of the fluctuative regime made

by von Oppen and Riedel⁵ for the single order parameter case, based on the Ginzburg–Landau energy functional. Further, we have made semi-analytic evaluations of the influence of fluctuations on the persistent current and on the order parameters in the ring, as functions of temperature, coupling between the order parameters, and magnetic flux. We have identified the ranges of parameters where fluctuations inhibit or enhance the persistent current in the ring, and pointed out the influence of the cross section of the ring as well as the influence of the freedom of the order parameters to undergo separate fluctuations. Although the influence of fluctuations is most important close to T_c , we have also studied the behavior far from T_c , providing a complete picture.

In addition to two-band materials, our findings apply to artificially made systems of two superimposed rings, as encountered in experiments that involve annular Joseph-

son junctions. The present study can also serve as a guideline for theoretical efforts and interpretations of experimental data in systems described by multiple order parameters in the fluctuative regime, especially in nanoscale samples, which are always effectively multiband due to quantum confinement¹⁵ and where fluctuations are of utmost importance.¹⁶

Acknowledgments

This research was supported by the Israel Science Foundation, grant 249/10, the Flemish Science Foundation (FWO-VI), and the ESF network INSTANS. We are grateful to Andrei Varlamov and Felix von Oppen for their answers to our enquiries.

-
- ¹ A. I. Larkin and A. A. Varlamov, *Theory of Fluctuations in Superconductors* (Oxford University Press, London, 2005).
- ² B. Rosenstein and D. Li, *Rev. Mod. Phys.* **82**, 109 (2010).
- ³ W. A. Little and R. D. Parks, *Phys. Rev. Lett.* **9**, 9 (1962).
- ⁴ N. C. Koshnick, H. Bluhm, M. E. Huber and K. A. Moler, *Science* **318**, 1440 (2007).
- ⁵ F. von Oppen and E. K. Riedel, *Phys. Rev. B* **46**, 3203 (1992).
- ⁶ G. Schwiete and Y. Oreg, *Phys. Rev. Lett.* **103**, 037001 (2009).
- ⁷ H. Bluhm, N. C. Koshnick, M. E. Huber, and K. A. Moler, *Phys. Rev. Lett.* **97**, 237002 (2006).
- ⁸ See e.g., A. Davidson, B. Dueholm, B. Kryger, and N. F. Pedersen, *Phys. Rev. Lett.* **55**, 2059 (1985); E. Kavousanaki, R. Monaco, and R. J. Rivers, *Phys. Rev. Lett.* **85**, 3452 (2000); A. V. Ustinov, C. Coqui, A. Kemp, Y. Zolotaryuk, and M. Salerno, *Phys. Rev. Lett.* **93**, 087001 (2004).
- ⁹ B.T. Geilikman, R.O. Zaitsev and V.Z. Kresin, *Soviet Physics - Solid State* **9**, 642 (1967) [*Fiz. Tverd. Tela* **9**, 821 (1967)].
- ¹⁰ M. E. Zhitomirsky and V.-H. Dao, *Phys. Rev. B* **69**, 054508 (2004).
- ¹¹ V. G. Kogan and J. Schmalian, *Phys. Rev. B* **83**, 054515 (2011).
- ¹² A. A. Shanenko, M. V. Milošević, F. M. Peeters, and A. V. Vagov, *Phys. Rev. Lett.* **106**, 047005 (2011).
- ¹³ D.J. Scalapino, M. Sears, and R.A. Ferrell, *Phys. Rev. B* **6**, 3409 (1972).
- ¹⁴ A. A. Golubov, J. Kortus, O. V. Dolgov, O. Jepsen, Y. Kong, O. K. Andersen, B. J. Gibson, K. Ahn, and R. K. Kremer, *J. Phys.: Condens. Matter* **14**, 1353 (2002).
- ¹⁵ Y. Guo, Y.-F. Zhang, X.-Y. Bao, T.-Z. Han, Z. Tang, L.-X. Zhang, W.-G. Zhu, E. G. Wang, Q. Niu, Z. Q. Qiu, J.-F. Jia, Z.-X. Zhao, and Q.-K. Xue, *Science* **306**, 1915 (2004); D. Eom, S. Qin, M.Y. Chou, and C. K. Shih, *Phys. Rev. Lett.* **96**, 027005 (2006).
- ¹⁶ W. V. Pogosov, *Phys. Rev. B* **81**, 184517 (2010); W. V. Pogosov, V. R. Misko, and F. M. Peeters, *Phys. Rev. B* **82**, 054523 (2010).
- ¹⁷ This is due to the fact that in the absence of fluctuations thermodynamic quantities are determined by the derivatives of F with respect to $r_{1,2}^2$, which in one case give $b_{1,2}r_{1,2}^2$ and in the other, the equivalent $b_{1,2}\langle r_{1,2}^2 \rangle$.